

Long-Term Strength and Damage Analysis of Laminated Composites

Yuris A. Dzenis*

University of Nebraska at Lincoln, Lincoln, Nebraska 68588-0347
and

Shiv P. Joshi†

University of Texas at Arlington, Arlington, Texas 76019-0018

A modified version of the probabilistic model developed by the authors for damage evolution analysis of laminates subjected to random loading is utilized to predict long-term strength of laminates. The model assumes that each ply in a laminate consists of a large number of mesovolumes. Probabilistic variation functions for mesovolumes stiffnesses as well as strengths are used in the analysis. Stochastic strains are calculated using the lamination theory and random function theory. Deterioration of ply stiffnesses is calculated on the basis of the probabilities of mesovolumes failures using the theory of excursions of random process beyond the limits. Long-term strength and damage accumulation in a Kevlar®/epoxy laminate under tension and complex in-plane loading are investigated. Effects of the mean level and stochastic deviation of loading on damage evolution and time to failure are discussed. It is found that the effect of the deviation in loading is more pronounced at lower mean loading levels. Long-term cumulative damage at the time of the final failure at low loading levels is higher than at high loading levels. The analytical results are qualitatively compared with the available experimental observations.

Introduction

BEHAVIOR of composites under long-term loading is of practical importance inasmuch as many composite structural elements are subjected to static loads. A number of empirical and semiempirical models describing creep rupture of composite laminates were developed in Refs. 1–4. The Ref. 4 model, for example, combines lamination theory and micromechanics with phenomenological equations for long-term strength of constituents and interfaces. However, these equations contain coefficients, which are not easy to obtain in experiments. Besides, these models do not take into account continuous nature of failure in composites. It is well known that the failure process in composite materials is a continuous process of initiation, accumulation, and evolution of damage at different structural levels. The progressive damage development is due to a number of random factors, such as random material properties of constituents, random composite microstructure, and random loading. Progressive damage development in composites under fatigue loading was observed by many researchers.^{5–7} Continuous development of damage in composites under long-term static loading was reported, for example, in Ref. 8. These and other observations suggest that prediction of long-term behavior of laminates should be based on a damage mechanics approach.

Recently, Allen et al.^{9–12} and Reifsnider et al.^{13–15} developed continuum damage mechanics models for laminated composites. These models introduced damage parameters that are internal state variables. Effects of accumulated damage on elastic and viscoelastic behavior of laminates were studied. Damage evolution laws were derived based on thermomechanics^{9–12} and kinetics^{13–15} considerations. These models adequately describe damage evolution in laminates under quasistatic and fatigue loads.

Another approach for damage analysis of laminates based on stochastic mechanics was developed in Refs. 16–19. This model explicitly accounts for stochastic factors and describes continuous damage evolution in laminates from nucleation to failure. The model is based on division of each layer into a statistically large number

of mesovolumes. Concentration of broken mesovolumes in plies is calculated as a probability of ply random strains to exceed the limiting failure strains. These concentrations are utilized in ply stiffness reduction. The model was applied to study laminate behavior under quasistatic loadings. Analytical predictions of the effect of the loading rate on damage evolution and deformation history are found to be in agreement with experimental data.¹⁸ In this paper, the approach^{16–19} is extended and modified to describe the damage evolution in laminates subjected to stationary long-term loading.

Problem Formulation

Consider a symmetric laminate consisting of unidirectionally reinforced plies with initial random elastic material properties

$$\tilde{E}_{1_0}^k \quad \tilde{E}_{2_0}^k \quad \tilde{G}_{12_0}^k \quad \text{and} \quad \tilde{\nu}_{12_0}^k$$

Here the tilde denotes random characteristics, and index k denotes ply number. We assume the normal distribution of laminas characteristics; therefore, we describe them by means of mathematical expectations

$$\bar{E}_{1_0}^k \quad \bar{E}_{2_0}^k \quad \bar{G}_{12_0}^k \quad \text{and} \quad \bar{\nu}_{12_0}^k$$

and dispersions

$$D_{E_{1_0}^k} \quad D_{E_{2_0}^k} \quad D_{G_{12_0}^k} \quad \text{and} \quad D_{\nu_{12_0}^k}$$

Laminate layup is described by ply orientation angles α^k . Loads applied to such a system results in a random stress-strain field in the laminas. Even under a very small applied loading, a nonzero probability of ply failure exists and damage starts to accumulate. Accumulation of damage causes reduction in laminas' material properties and stress redistribution between plies.

Assume that the stresses applied $\tilde{\sigma}(t) = [\tilde{\sigma}_1(t), \tilde{\sigma}_2(t), \tilde{\tau}_{12}(t)]$ are independent stationary Gaussian processes of time. It means that these processes can be described by mathematical expectations $\bar{\sigma}$ and correlation functions $K_{\tilde{\sigma}}(t_1, t_2) = K_{\tilde{\sigma}}(t_2 - t_1) = K_{\tilde{\sigma}}(\delta)$. The derivatives of stresses will also be stationary processes with zero mathematical expectations and correlation functions defined as follows:

$$K_{\dot{\tilde{\sigma}}}(\delta) = -\frac{d^2}{d\delta^2} K_{\tilde{\sigma}}(\delta) \quad (1)$$

Application of these stresses to a laminate creates random deformation and stress functions in plies $\tilde{\epsilon}_i^k(t)$ and $\tilde{\sigma}_i^k(t)$, respectively.

Received Jan. 5, 1996; revision received Jan. 28, 1997; accepted for publication Feb. 9, 1997. Copyright © 1997 by the American Institute of Aeronautics and Astronautics, Inc. All rights reserved.

*Assistant Professor, Center for Materials Research and Analysis, Department of Engineering Mechanics. Member AIAA.

†Professor, Center for Composite Materials, Department of Mechanical and Aerospace Engineering. Member AIAA.

We have to assess the probability of random strain functions $\tilde{\varepsilon}_i^k(t)$ in each ply to exceed the limiting bounds $\tilde{\varepsilon}_i^k$ and $\tilde{\varepsilon}_i^k$, where the positive $\tilde{\varepsilon}_i^k$ (in tension) and negative $\tilde{\varepsilon}_i^k$ (in compression) strengths are random in general. This probability can be calculated as

$$r_i^k(t) = 1 - \exp\left(-\int_0^t v_i^k(\tau) d\tau\right) \quad (2)$$

where $v_i^k(t)$ is the mathematical expectation of a number of excursions of $\tilde{\varepsilon}_i^k(t)$ beyond the interval $[\tilde{\varepsilon}_i^k, \tilde{\varepsilon}_i^k]$ per unit time.¹⁸ Assuming statistical independence of crossing the negative and positive bounds, $v_i^k(t)$ can be calculated as a sum of mathematical expectations of these events,

$$v_i^k(t) = v_{i-}^k(t) + v_{i+}^k(t) \quad (3)$$

The mathematical expectation of the number of excursions beyond the negative and positive limits can be calculated¹⁸ as

$$\begin{aligned} v_{i-}^k(t) &= \frac{1}{2\pi} \sqrt{\frac{D_{\varepsilon_i}}{D_{\varepsilon_i} + D_{\varepsilon_l}}} \exp\left(-\frac{[\tilde{\varepsilon}_i(t) - \tilde{\varepsilon}_l]^2}{2(D_{\varepsilon_i} + D_{\varepsilon_l})}\right) \\ &\times \left\{ \exp\left(-\frac{\tilde{\varepsilon}_i(t)^2}{2D_{\varepsilon_i}}\right) - \sqrt{\frac{2\pi}{D_{\varepsilon_i}}} \tilde{\varepsilon}_i(t) \Phi\left(-\frac{\tilde{\varepsilon}_i(t)}{\sqrt{D_{\varepsilon_i}}}\right) \right\} \\ v_{i+}^k(t) &= \frac{1}{2\pi} \sqrt{\frac{D_{\varepsilon_i}}{D_{\varepsilon_i} + D_{\varepsilon_l}}} \exp\left(-\frac{[\tilde{\varepsilon}_i(t) - \tilde{\varepsilon}_l]^2}{2(D_{\varepsilon_i} + D_{\varepsilon_l})}\right) \\ &\times \left\{ \exp\left(-\frac{\tilde{\varepsilon}_i(t)^2}{2D_{\varepsilon_i}}\right) + \sqrt{\frac{2\pi}{D_{\varepsilon_i}}} \tilde{\varepsilon}_i(t) \left[1 - \Phi\left(-\frac{\tilde{\varepsilon}_i(t)}{\sqrt{D_{\varepsilon_i}}}\right)\right] \right\} \end{aligned} \quad (4)$$

where

$$\Phi(U) = \frac{1}{\sqrt{2\pi}} \int_{-\infty}^U e^{-(u^2/2)} du = \frac{1}{2} \left[1 + \operatorname{erf}\left(\frac{U}{\sqrt{2}}\right) \right]$$

is a Laplace function; the ply index k is dropped for simplicity. To use the formulas (4) we need to have the following information about the ply strains: $\tilde{\varepsilon}_i^k(t)$, $\tilde{\varepsilon}_i^k$, and $D_{\varepsilon_i^k}$. Note that the simple relationship (2) between the probability of event and mathematical expectation of the number of events assumes the Poisson type process of event formations with time. This can be valid for rare independent events. In our case, the use of the formula is justified if the average time spacing between the occurrence of events is larger than the autocorrelation time for the loading process.

The mathematical expectations and dispersions of laminate deformations and deformation derivatives can be calculated using the properties of random function operators,

$$\begin{aligned} \bar{\varepsilon}_i(t) &= \bar{\varepsilon}_{i0} + \bar{\sigma}_j \int_0^t \bar{S}_{ij}(\tau) d\tau & \bar{\varepsilon}_i(t) &= \bar{S}_{ij}(t) \bar{\sigma}_j \\ D_{\varepsilon_i} &= \bar{S}_{ij}^2(t) K_{\sigma_j}(0) + \bar{\sigma}_j^2 D_{S_{ij}} \\ D_{\varepsilon_i} &= \bar{S}_{ij}^2(t) K_{\sigma_j}(0) + \bar{S}_{ij}^2(t) K_{\sigma_j}(0) \end{aligned} \quad (5)$$

One needs to relate the failure probability [Eq. (2)] to damages of different types and their effect on the current mechanical properties of the composite. Assume that there are three types of damages related to three in-plane deformations in each ply $\varepsilon_i^k = [\varepsilon_{11}^k, \varepsilon_{22}^k, \gamma_{12}^k]$. Failure type due to ε_{11}^k exceeding the critical bound can be associated with fiber breakage, and those due to ε_{22}^k and γ_{12}^k can be associated with matrix cracking in transverse to fiber direction and in shear, respectively.

Assume that each ply consists of a large number of mesovolumes containing a sufficient amount of reinforcing fibers to satisfy the condition of stochastic homogeneity. Initial material properties distributions of a ply are considered to be equal to the respective mesovolumes characteristics. Assume that each of the mesovolumes can be either perfect or broken in any of three ways, namely, in fiber

direction, in transverse direction, and in shear. Therefore, we can suppose that at the current state of loading, the relative numbers of broken mesovolumes in plies for each type of failure are proportional to probabilities of failure r_i^k . In the limiting case of the infinite number of mesovolumes in ply, the proportionality becomes equality. Thus, we can interpret the numbers $r_i^k = [r_{11}^k, r_{22}^k, r_{12}^k]$ as relative counts of broken mesoelements of three types in each ply.

Accumulation of damages in composite laminas causes stiffness reduction of laminate and stress redistribution around the microcracks and between the plies. This process is very complicated, and modeling damage accumulation using microlevel consideration is, in general, not amenable to analytical studies.

It is assumed that mesoelement failure in a certain direction causes deterioration of properties in the same direction. Failure of the r_i^k fraction of all mesoelements in i th direction of k th ply will result in reduction of ply elastic modulus in this direction. It is proposed that mathematical mean values of ply elastic moduli decrease with damage accumulation as follows:

$$\begin{aligned} \bar{E}_1^k(\tau) &= \bar{E}_{10}^k [1 - r_{11}^k(\tau)] & \bar{E}_2^k(\tau) &= \bar{E}_{20}^k [1 - r_{22}^k(\tau)] \\ \bar{G}_{12}^k(\tau) &= \bar{G}_{120}^k [1 - r_{12}^k(\tau)] & \bar{\nu}_{12}^k(\tau) &= \bar{\nu}_{120}^k [1 - r_{11}^k(\tau)] \end{aligned} \quad (6)$$

but that relative standard deviations remain constant:

$$\begin{aligned} \frac{\sqrt{D_{E_1^k(\tau)}}}{E_1^k(\tau)} &= \frac{\sqrt{D_{E_{10}^k}}}{E_{10}^k} & \frac{\sqrt{D_{E_2^k(\tau)}}}{E_2^k(\tau)} &= \frac{\sqrt{D_{E_{20}^k}}}{E_{20}^k} \\ \frac{\sqrt{D_{G_{12}^k(\tau)}}}{G_{12}^k(\tau)} &= \frac{\sqrt{D_{G_{120}^k}}}{G_{120}^k} & \frac{\sqrt{D_{\nu_{12}^k(\tau)}}}{\nu_{12}^k(\tau)} &= \frac{\sqrt{D_{\nu_{120}^k}}}{\nu_{120}^k} \end{aligned} \quad (7)$$

According to this hypothesis, damage accumulation in the ply during laminate loading evokes the shift of ply moduli distributions toward the zero direction and narrows these distributions proportionally to stiffness decrease. This simple approach does not take into consideration micromechanical phenomena such as stress redistribution around the single cracks or cracks interaction, but does take into account gradual stiffness reduction due to damage accumulation in plies and stress redistribution between them.

Algorithmic Development

A computer code for laminate analysis under quasistatic loading is modified to investigate the laminate behavior under stationary loading. Initial laminate deformations $\bar{\varepsilon}_{i0}$ and damage functions after the load application are calculated using a deterministic loading approach.¹⁶ The time is increased incrementally in the program, and the deformation integral (5) is integrated numerically. At each time step, the damage functions $r_i^k(t)$, the current composite compliances, and the compliance derivatives from the previous step are used to calculate the laminate deformations. It is assumed that complete failure of a laminate occurs when any of the current effective elastic moduli, $\bar{E}_1(t)$, $\bar{E}_2(t)$, or $\bar{G}_{12}(t)$, becomes equal to zero. The calculated information for each time step is appended to the data file, including the information on laminate and laminas strains, the damage content $r_i^k(t)$ in plies, the average content of damages of different type in the laminate

$$r_i(t) = \sum_{k=1}^n \frac{r_i^k(t)}{n}$$

the cumulative damage content

$$r_c(t) = \sum_{i=1}^3 \frac{r_i(t)}{3}$$

and the current laminate elastic moduli $\bar{E}_1(t)$, $\bar{E}_2(t)$, $\bar{G}_{12}(t)$. The program is written in Mathematica language.

Analysis and Results

A numerical study of the effects of the loading level and dispersion on damage evolution in Kevlar[®]/epoxy [0/+30/90]_s laminate is performed. Experimental statistical data for Kevlar/epoxy unidirectional composite presented in Ref. 18 are used for the mesovolume

material properties definition (see discussion on mesovolume properties in Refs. 16 and 17).

The cases of tension $\tilde{\sigma}(t) = \{\tilde{\sigma}(t), 0, 0\}$ and complex in-plane loading $\tilde{\sigma}(t) = \{\tilde{\sigma}(t), \tilde{\sigma}(t), \tilde{\sigma}(t)\}$ of a laminate are analyzed. The mathematical expectation $\bar{\sigma}$ of the loading function is constant, and the correlation function of process is

$$K_{\sigma}(\delta) = \sigma_q^2 \exp(-\delta / \tau_0^2) \quad (8)$$

where $\sigma_q^2 = D_{\sigma} = K_{\sigma}(0)$ is dispersion of the process and τ_0 is autocorrelation time of random fluctuations of loading. The derivative $\dot{\tilde{\sigma}}(t)$, consequently, will have zero mathematical expectation and dispersion $D_{\dot{\tilde{\sigma}}} = \dot{K}_{\sigma}(0) = 2\sigma_q^2 / \tau_0^2$. The load levels are varied within an interval 0.2–0.6 of the deterministic strength of material σ calculated by Ref. 16. The following values of standard deviation of loading process σ_q are covered in the numerical study: 0.1, 1, 5, and 10 MPa. The correlation time was constant throughout calculations. Dimensionless time (time to correlation time ratio) was used in data analysis. In all cases, the time step in numerical integration was chosen to be $\sim \frac{1}{50}$ of time to failure.

Tension

Figure 1 shows the deformation behavior of $[0/_{\pm}30/90]_s$ laminate under uniaxial tension at loading level $\bar{\sigma} = 0.5\sigma$ with loading deviation $\sigma_q = 1$ MPa. A variation of damage functions r_i^k in the plies is shown in Fig. 2. Variation of average damage functions r_i and cumulative damage function r_c for the same loading case is shown in Figs. 3 and 4. In these, and in several of the following figures, continuous lines, dashed lines, and dash-dot lines correspond to 11, 22, and 12 components of the variables, respectively. The analysis shows that laminate failure begins with 90-deg ply failure in the transverse direction during initial load application. Then, from the very beginning of the test, shear failures start to accumulate in all plies (Fig. 2). The rate of shear damage accumulation is higher for ± 30 -deg plies. At some point during loading, fibers break due to compression in 90 ply (Fig. 2c), which causes fast transverse damage development in ± 30 plies and fiber damage in 0 ply (Figs. 2a and 2b) and leads to a final failure of the laminate. Laminate strains increase slowly up to 95% of time to failure and, subsequently, undergo a very fast increase before the final failure (Fig. 1). Average longitudinal (fiber and transverse matrix) damages remain practically unchanged up to 80% of all possible shear damage accumulation (Fig. 3). In the tensile loading case, the dominating failure accumulation mechanism is shear, but the final composite failure is governed by the fiber breakage in 90- and 0-deg plies (Figs. 3 and 4).

Complex Loading

Figure 5 shows deformation behavior of $[0/_{\pm}30/90]_s$ laminate under complex in-plane loading at a loading level $\bar{\sigma} = 0.5\sigma$ with loading deviation $\sigma_q = 5$ MPa. Variation of damage functions r_i^k in the plies is shown in Fig. 6. Note that due to the shear component of the applied loading, the deformations and, consequently, the damage functions for 30- and ± 30 -deg plies are different (Figs. 6b and 6c). Variation of average damage functions r_i and cumulative damage function r_c for this loading case is shown in Figs. 7 and 8. It is observed (Fig. 6) that matrix transverse failure occurs in 0 and ± 30

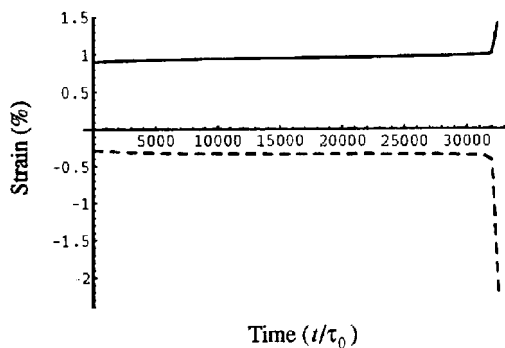


Fig. 1 Deformation of $[0/_{\pm}30/90]_s$ laminate under uniaxial tension.

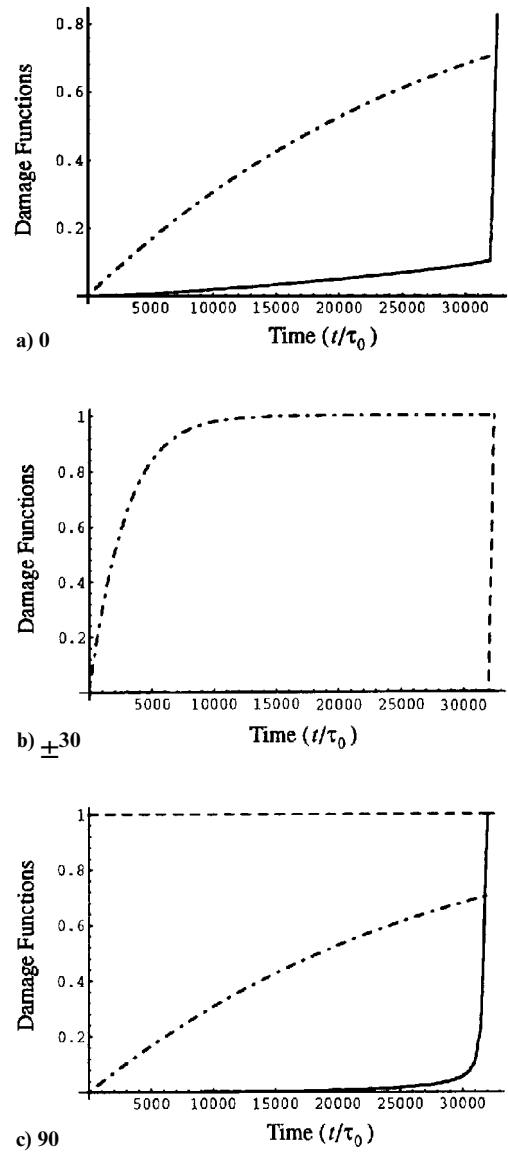


Fig. 2 Damage formation in plies of $[0/_{\pm}30/90]_s$ laminate under uniaxial tension.

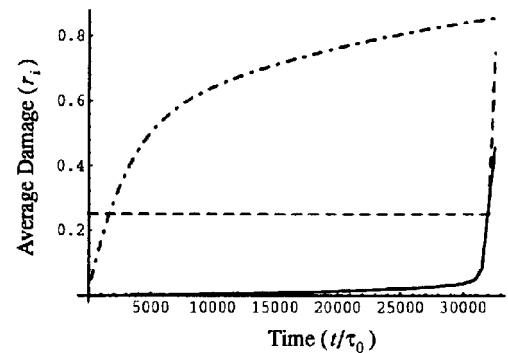


Fig. 3 Average damage formation in $[0/_{\pm}30/90]_s$ laminate under uniaxial tension.

plies during the initial load application. As in the previous loading case, shear damage starts to develop in all plies from the beginning of the test. The rate of shear damage accumulation is higher for the 0- and 90-deg plies and is very low for the ± 30 -deg ply. The first fiber breakage occurs at about 70% of the time to failure in the ± 30 -deg ply (Fig. 6c) and is followed by an accelerated shear damage development in the other plies. A final laminate failure occurs when the fibers start to break in the 30- and 0-deg plies. Unlike

the tensile loading case, laminate strains start to change rapidly after about 75% of the time to failure (Fig. 5). The dominating failure in the accumulation mechanism is again shear (Fig. 7), but a small amount of fiber failure is observed under complex loading as early as at about the 50% of the time to failure. The final failure development for this loading case is more gradual and over a larger relative time interval (Fig. 8). Calculations without accounting for initial damage showed that for the complex loading, initial damage

is important and, if not accounted for in the calculations, may lead to an overestimation of the time to failure up to 25%. Dominating gradual shear failure at early loading stages for both loading cases is due to the high shear failure strain scatter for Kevlar/epoxy unidirectional composite (31% according to experimental data). It causes an existence of a nonzero failure probability long before the average shear deformation in plies reaches an average failure strain.

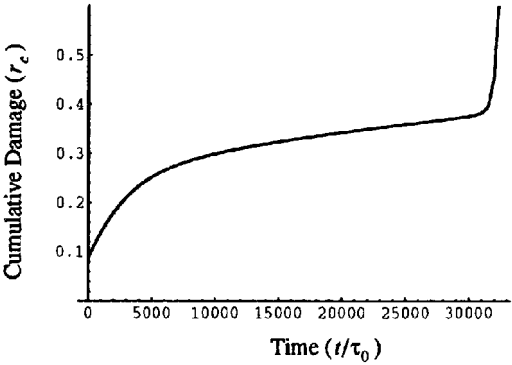


Fig. 4 Total damage formation in $[0/\pm 30/90]_s$ laminate under uniaxial tension.

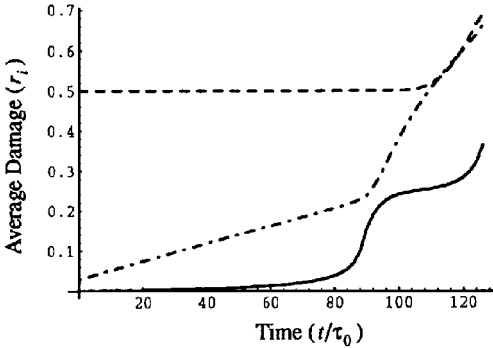


Fig. 7 Average damage formation $[0/\pm 30/90]_s$ laminate under complex loading.

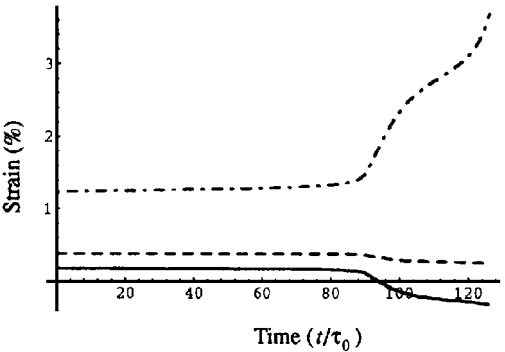


Fig. 5 Deformation of $[0/\pm 30/90]_s$ laminate under complex loading.

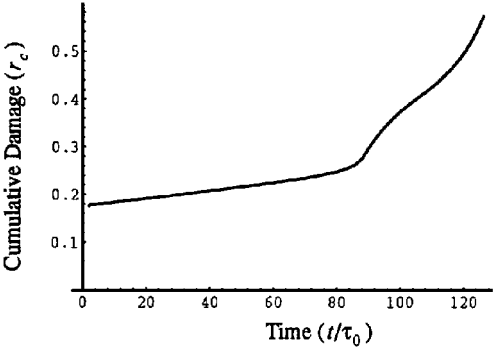
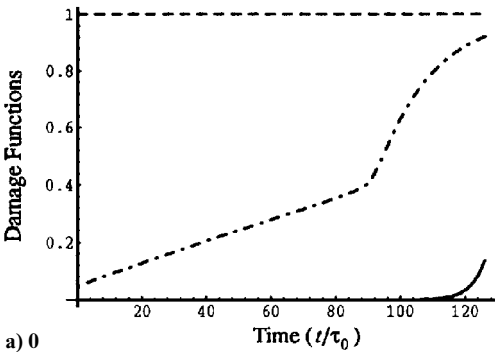
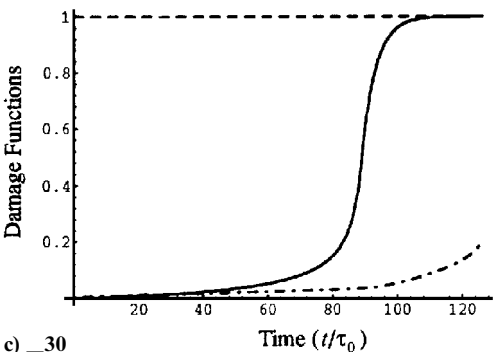


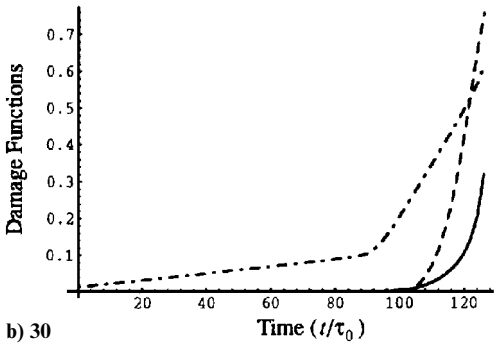
Fig. 8 Total damage formation $[0/\pm 30/90]_s$ laminate under complex loading.



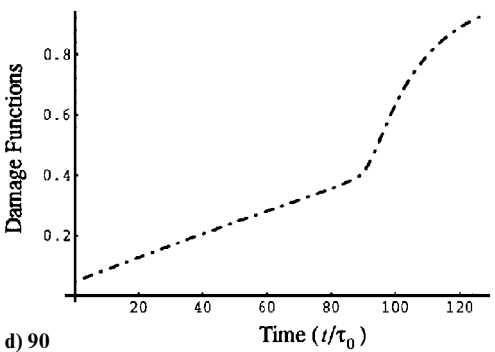
a) 0



c) -30



b) 30



d) 90

Fig. 6 Damage formation in plies of $[0/\pm 30/90]_s$ laminate under complex loading.

Effect of Loading Level

Total damage accumulation under uniaxial tension is shown in Fig. 9 for the four different loading levels: $\bar{\sigma} = 0.3, 0.4$, and 0.5 and 0.6σ . Average damage functions for these loading cases are shown in Fig. 10. It is seen that damage accumulation occurs over the longer time period at low-load levels. The cumulative damage content at the final failure is progressively increased from 0.56 to 0.93 with the decrease in the loading level from 0.6 to 0.3 (Fig. 9). It is due to a higher fiber and shear damage contents at the final failure for

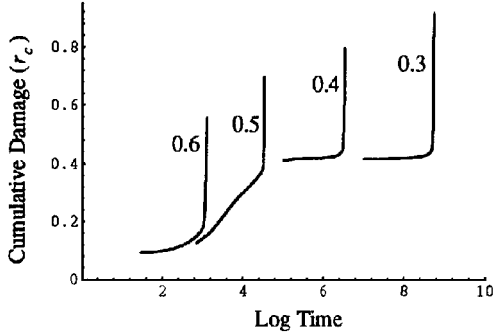
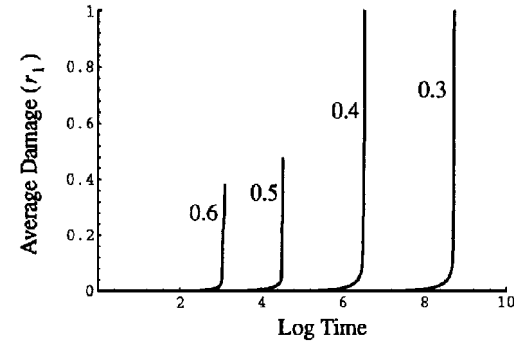
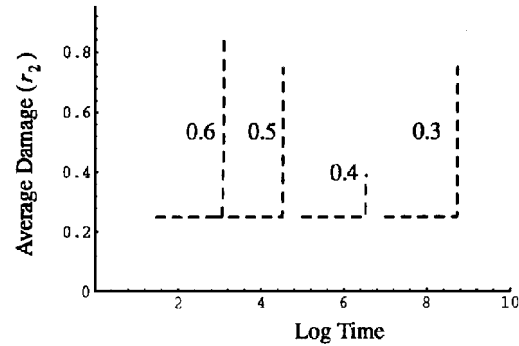


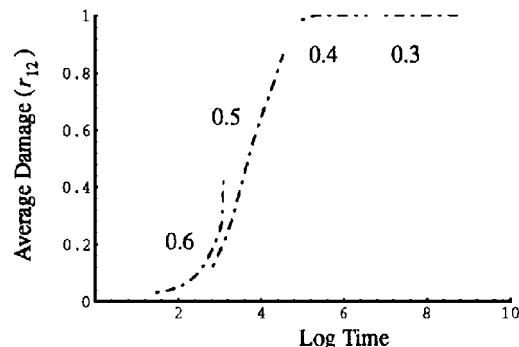
Fig. 9 Total damage formation in $[0/\pm 30/90]_s$ laminate under uniaxial tension at various loading levels, $\sigma_q = 1$ MPa.



a) Fiber damage



b) Transverse damage



c) Shear damage

Fig. 10 Average damage formation in $[0/\pm 30/90]_s$ laminate under uniaxial tension.

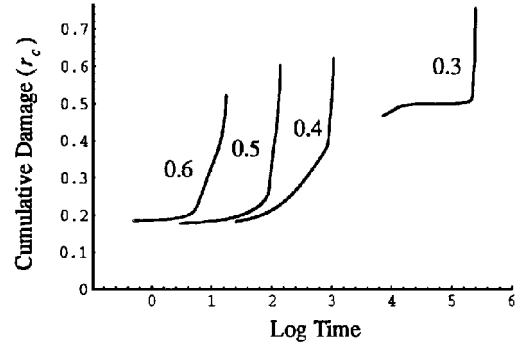


Fig. 11 Total damage formation in $[0/\pm 30/90]_s$ laminate under complex loading at various loading levels, $\sigma_q = 5$ MPa.

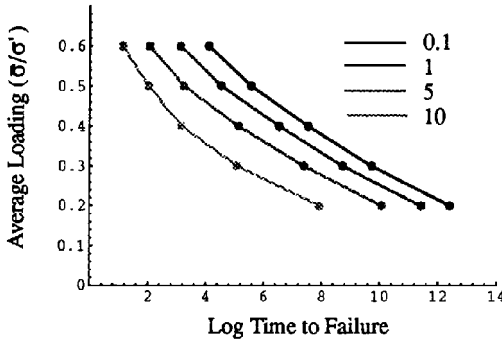
the low loads (Figs. 10a and 10c). Note that higher ultimate damage content under lower long-term loads was experimentally observed in Refs. 5, 20, and 21. Higher damage content before the final sharp increase in the damage for the lower loads (Fig. 9) is due to the significant shear damage accumulation during the first time increment of the loading, which is not shown in Fig. 9. Approximately 50 time increments to final failure are used in the numerical calculations, and the curves are plotted on a logarithmic time scale. The time to failure increases considerably with the decrease in the loading level. Substantial transverse matrix damage, seen in Fig. 10b, occurs in the 90-deg ply during the initial load application. At low loading levels, complete shear damage is developed in the composite during the first time step (Fig. 10c). The fiber damage accumulation in all of the plies is insignificant until just before the final failure (Fig. 10a). Thus, the final failure in all cases is governed by the onset of fiber damage.

Total damage accumulation under complex loading is shown in Fig. 11 for four loading levels. Note that the deviation of loading is higher. Qualitatively similar behavior is observed as evident from the comparison of Figs. 9 and 11. The cumulative damage content at final failure increases from 0.52 to 0.75 with the decrease in loading from 0.6 to 0.3σ . In this case, also, shear damage tends to develop at the beginning of the loading process as the loading level decreases. It reveals as an apparent higher initial damage content for lower loading levels (Fig. 11).

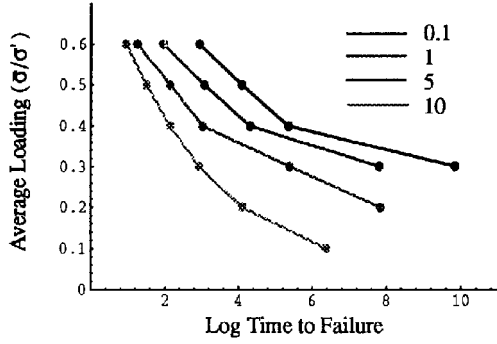
For both tensile and complex loading, a further decrease of average applied loading leads to the development of computational instability. At low loadings and small loading deviations, the very large exponents in Eqs. (2) and (4) produce unreliable numerical results. The lower load limits for this method, evaluated by numerical analysis, are found to be 20–25% of the deterministic strength of the laminates. The current theory is not applicable for lower loadings. Note, however, that long-term loads of practical interest are usually higher than 25% of the static strength of materials.

Effect of Loading Deviation

The variations of the time to failure with the average loading level under tension and complex loading are shown in Figs. 12a and 12b, respectively, for the four different values of the loading deviation. It is seen that the increase of loading scatter decreases the time to failure. This effect is more pronounced for the low loadings. For example, the increase of scatter from 0.1 to 10 MPa causes a decrease of the time to failure under the complex loading level 0.6σ of about two orders of magnitude. However, at the loading level 0.3σ the same increase in scatter produces a decrease of the time to failure of seven orders of magnitude. When loaded in tension, the time to failure on a logarithmic scale varies gradually with the loading level, whereas under the complex loading there is a distinguishable kink at $\bar{\sigma}$ about 0.4 of deterministic strength σ . Similar kinks were experimentally observed on fatigue curves of composite laminates, for example, in Ref. 22. The mechanisms of this behavior were not discussed. The analysis of deterministic damage evolution under the complex loading shows that the matrix transverse damage develops at this load in the 0-deg ply. Thus, damage development during initial load application under quasistationary loading, or damage



a) Tension



b) Complex loading

Fig. 12 Variation of time to failure with average loading levels, where numbers indicate deviation of loading in megapascal.

development during the first loading cycle under fatigue, may be responsible for the change of slope of the stress-life curves.

Effect of Laminate Creep Due to Damage: Comparison with Stationary Limit

The preceding analysis is performed using the full quasistationary problem formulation, Eqs. (2–5). According to this formulation, the mean strains in the laminate and plies change because of a gradual stiffness degradation due to damage, even though the applied mean loading is constant in time. The problem can be substantially simplified by neglecting nonstationary effects. Assuming that the processes of changing the composite compliances are slow and their derivatives may be neglected, formulas (4) and (5) can be reduced to

$$v_{i-} = \frac{1}{2\pi} \sqrt{\frac{D_{\bar{\epsilon}_i}}{D_{\bar{\epsilon}_i} + D_{\bar{\epsilon}_j}}} \exp \left[-\frac{(\bar{\epsilon}_i - \bar{\epsilon}_j)^2}{2(D_{\bar{\epsilon}_i} + D_{\bar{\epsilon}_j})} \right] \quad (9)$$

$$v_{i+} = \frac{1}{2\pi} \sqrt{\frac{D_{\bar{\epsilon}_i}}{D_{\bar{\epsilon}_i} + D_{\bar{\epsilon}_j}}} \exp \left[-\frac{(\bar{\epsilon}_i - \bar{\epsilon}_j)^2}{2(D_{\bar{\epsilon}_i} + D_{\bar{\epsilon}_j})} \right] \quad (10)$$

$\bar{\epsilon}_i = \bar{\epsilon}_{i0} \quad \bar{\epsilon}_j = 0$

$$D_{\bar{\epsilon}_i} = \bar{S}_{ij}^2(t) K_{\sigma_j}(0) + \bar{\sigma}_j^2 D_{S_{ij}} \quad D_{\bar{\epsilon}_i} = \bar{S}_{ij}^2(t) K_{\sigma_j}(0)$$

Formulations (9) and (10) represent a stationary limit for this problem. The variations of the time to failure in the two cases of tensile and complex loading, which were calculated using this stationary formulation, are compared with the results obtained by utilizing Eqs. (4) and (5) in Fig. 13. It is observed that neglecting the damage-induced changes in laminate compliances and, consequently, neglecting the changes in laminate and ply strains leads to a considerable overestimation of the time to failure. This effect is more pronounced at lower loads. The difference increases more rapidly with the decrease of mean loading level in the case of complex loading (Fig. 13b). Thus, the simplified formulation [Eqs. (9) and (10)] may lead to a significant overestimation of the

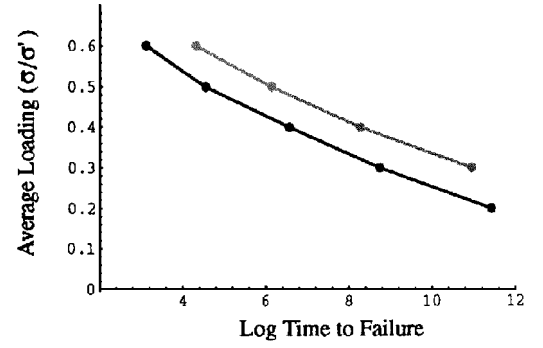
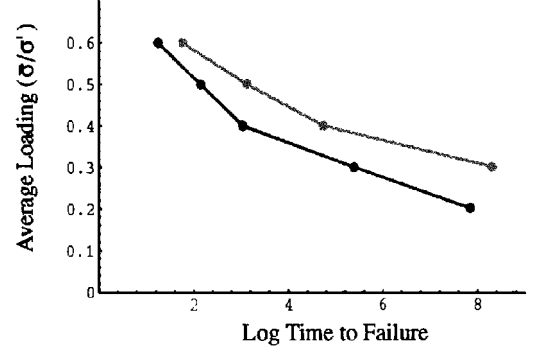
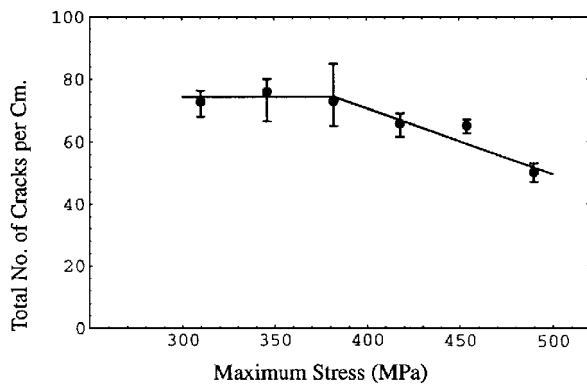
a) Tension, $\sigma_q = 1$ MPab) Complex loading, $\sigma_q = 5$ MPa

Fig. 13 Variation of time to failure with average loading level, where black is full formulation [Eqs. (4) and (5)] and gray is simplified formulation [Eqs. (9) and (10)].

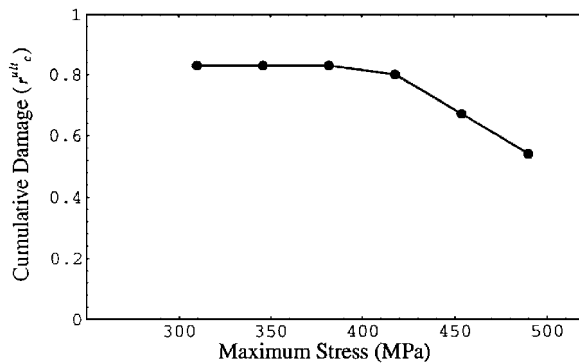
laminate life. It is interesting to note that the stationary formulation predicts the same shapes of the stress-life curves as the full formulation (the smooth curve in tension and the kinked one in complex loading).

Damage Content at Failure: Comparison with Experimental Observations

Experimental observation of the variation of damage content at failure in composites under long-term fatigue loading was performed in Ref. 20. An ultimate crack density in a quasi-isotropic $[0/90/_{\pm 45}]_s$ graphite/epoxy laminate was evaluated by counting the total number of cracks at failure. Experimental results for six loading amplitudes and their empirical approximation²⁰ are shown in Fig. 14a. The stochastic material property data are not available for the material used in the experimental investigation. A qualitative comparison of these experimental observations with model predictions was performed using available properties of a Fiberite® T300 graphite/epoxy composite. The following mean stiffness and strength data were used in calculations: $E_1 = 133$ GPa, $E_2 = 9.3$ GPa, $G_{12} = 5.4$ GPa, $\nu_{12} = 0.34$, $\epsilon_1 = 0.011$, $\epsilon_2 = -0.0033$, $\epsilon_3 = 0.0064$, $\epsilon_4 = -0.013$, and $\gamma_{12} = |\gamma_{12}^c| = 0.048$. The stochastic variance of the stiffness data was assumed to be 5%. The variance of the strength data was 8%. The analysis was performed using the stochastic model described earlier modified for a fatigue loading.²³ The damage accumulation in a $[0/90/_{\pm 45}]_s$ laminate under long-term cyclic tension was studied in the maximum stress interval from 310 to 490 MPa, that is, approximately 0.4–0.6 of the deterministic strength of this material as calculated by Ref. 16. The loading deviation was 5 MPa. Predicted ultimate cumulative damage at failure is shown in Fig. 14b. The qualitative comparison between the theoretical and experimental results is quite good. The model correctly predicts the increase in the ultimate damage content with the load decrease, as well as the saturation of this trend for lower loads. Although this is a very limited comparison, the results are very encouraging. An agreement between the experimental and theoretical data assures that final failure in composites under long-term loading develops as a result of damage evolution.



a) Experimental data and empirical approximation²⁰



b) Theoretical results by a modified stochastic model²³

Fig. 14 Comparison of ultimate damage content at fatigue failure between the experimental observations and the modified theoretical model for a graphite/epoxy $[0]_{\pm 45/90}_s$ laminate.

Conclusions

A probabilistic model utilizing random material characteristics to predict damage evolution in laminated composites under long-term loading has been presented. A numerical algorithm for damage accumulation and deformation history predictions for laminates has been developed. Behavior of a Kevlar/epoxy laminate subjected to tension and complex in-plane loading was presented as an illustrative example. The effects of the mean loading level and the deviation on the damage accumulation and time to failure were discussed. Two phenomena, the characteristic kinks on the stress-life curves of some laminates and the higher cumulative damage content at failure for lower load levels, were captured by the developed model for the first time theoretically. The analytical predictions qualitatively corroborate with the available experimental data.

Acknowledgments

Y. A. Dzenis acknowledges the support provided for this research by the U.S. Air Force Office of Scientific Research, Grant F49620-96-1-0458, and the Nebraska Research Initiative Grant of the College of Engineering and Technology, University of Nebraska at Lincoln.

References

- ¹Gerstle, F. P., Jr., and Kunz, S. C., "Prediction of Long-Term Failure in Kevlar 49 Composites," *Long-Term Behavior of Composites*, American Society for Testing and Materials, Philadelphia, PA, 1983, pp. 263–292 (ASTM STP 813).
- ²Kemmochi, K., Koshizaki, N., Hojo, M., Takayanagi, H., Nagasawa, C., and Hayashi, R., "A Study of Life Due to Creep Behavior in CF/Epoxy and CF/PEEK Laminates," *Advanced Composite Materials*, 1st France-Japan Seminar on Composite Materials, SIRPE, Paris, 1990, pp. 211–218.
- ³Dillard, A. D., and Brinson, H. F., "A Numerical Procedure for Predicting Creep and Delayed Failures in Laminated Composites," *Long-Term Behavior of Composites*, American Society for Testing and Materials, Philadelphia, PA, 1983, pp. 23–37 (ASTM STP 813).

- ⁴Skudra, A. M., and Gurvich, M. R., "Structural Theory of the Long-Term Strength of Reinforced Plastics," *Mechanics of Composite Materials*, Vol. 26, No. 5, 1990, pp. 833–839.
- ⁵Reifsnider, K. L., Shulte, K., and Duke, J. C., "Long-Term Fatigue Behavior of Composite Materials," *Long-Term Behavior of Composites*, edited by T. K. O'Brien, American Society for Testing and Materials, Philadelphia, PA, 1983, pp. 136–159 (ASTM STP 813).
- ⁶Jamison, R. D., Shulte, K., Reifsnider, K. L., and Stinchcomb, W. W., "Characterization and Analysis of Damage Mechanisms in Tension-Tension Fatigue of Graphite-Epoxy Laminates," *Effects of Defects in Composite Materials*, American Society for Testing and Materials, Philadelphia, PA, 1984, pp. 21–55 (ASTM STP 813).
- ⁷Reifsnider, K. L. (ed.), *Fatigue of Composite Materials*, Elsevier, London, 1991.
- ⁸Rochat, N., Fougères, R., and Fleishmann, P., "Delayed Acoustic Emission—A Rheological Approach," *3rd International Symposium on Acoustic Emission from Composite Materials*, American Society for Non-destructive Testing, Columbus, OH, pp. 184–193.
- ⁹Allen, D. H., Harris, C. E., and Groves, S. E., "A Thermomechanical Constitutive Theory for Elastic Composites with Distributed Damage—Part I: Theoretical Development," *International Journal of Solids and Structures*, Vol. 23, No. 4, 1987, pp. 1301–1318.
- ¹⁰Allen, D. H., Harris, C. E., and Groves, S. E., "A Thermomechanical Constitutive Theory for Elastic Composites with Distributed Damage—Part II: Application to Matrix Cracking in Laminated Composites," *International Journal of Solids and Structures*, Vol. 23, No. 9, 1987, pp. 1319–1338.
- ¹¹Allen, D. H., Groves, S. E., and Harris, C. E., "A Cumulative Damage Model for Continuous Fiber Composite Laminates with Matrix Cracking and Interply Delamination," *Composite Materials: Testing and Design*, American Society for Testing and Materials, Philadelphia, PA, 1988, pp. 57–80 (ASTM STP 972).
- ¹²Allen, D. H., Highsmith, A. L., and Lo, D. C., "A Continuum Damage Mechanics Model for Life Prediction of Laminated Composites," *Durability of Polymer Based Composite Systems for Structural Applications*, Elsevier, London, 1991, pp. 119–128.
- ¹³Reifsnider, K. L., and Stinchcomb, W. W., "A Critical Element Model of the Residual Strength and Life of Fatigue-Loaded Composite Coupons," *Composite Materials: Fatigue and Fracture*, American Society for Testing and Materials, Philadelphia, PA, 1986, pp. 298–313 (ASTM STP 907).
- ¹⁴Reifsnider, K. L., "Use of Mechanistic Life Prediction Methods for the Design of Damage Tolerant Composite Material Systems," American Society for Testing and Materials, Philadelphia, PA, 1992, pp. 205–223 (ASTM STP 1157).
- ¹⁵Reifsnider, K. L., Lesco, J., and Case, S., "Kinetic Methods for Prediction of Damage Tolerance of High Temperature Polymer Composites," *COMPOSITES'95: Recent Advances in Japan and the United States* (Kyoto, Japan), Japan Society for Composite Materials, Tokyo, Japan, 1995, pp. 49–56.
- ¹⁶Dzenis, Y. A., Joshi, S. P., and Bogdanovich, A. E., "Damage Evolution Modeling in Orthotropic Laminated Composites," *AIAA Journal*, Vol. 32, No. 2, 1994, pp. 357–364.
- ¹⁷Dzenis, Y. A., Bogdanovich, A. E., and Pastore, C. M., "Stochastic Damage Evolution in Textile Laminates," *Composites Manufacturing*, Vol. 4, No. 4, 1993, pp. 187–194.
- ¹⁸Dzenis, Y. A., Joshi, S. P., and Bogdanovich, A. E., "Behavior of Laminated Composites Under Monotonically Increasing Random Load," *AIAA Journal*, Vol. 31, No. 12, 1993, pp. 2329–2334.
- ¹⁹Dzenis, Y. A., and Joshi, S. P., "Damage Induced Anisotropy in Laminates," *Advanced Composites Letters*, Vol. 2, No. 3, 1993, pp. 97–99.
- ²⁰Kim, R. Y., "Experimental Assessment of Static and Fatigue Damage of Graphite/Epoxy Laminates," *Advances in Composite Materials*, Vol. 2, edited by A. R. Bunsell, C. Bathias, A. Martrenchar, D. Menkes, and G. Verchery, Pergamon, New York, 1980, p. 1015.
- ²¹Jen, M.-H. R., Kau, Y. S., and Wu, I. C., "Fatigue Damage in Centrally Notched Composite Laminate Due to Two-Step Spectrum Loading," *Fatigue*, Vol. 16, April 1994, pp. 193–201.
- ²²Boller, K. H., "Fatigue Characteristics of RP Laminates Subjected to Axial Loading," *Modern Plastics*, Vol. 41, 1964, p. 145.
- ²³Dzenis, Y. A., "Fatigue Damage Analysis of Composites: A Novel Approach," *COMPOSITES'95: Recent Advances in Japan and the United States*, Proceedings of the Seventh Japan-U.S. Conf. on Composite Materials, edited by I. Kimpara, H. Miyairi, and N. Takeda, Japan Society for Composite Materials, Kyoto, Japan, 1995, pp. 561–567.

G. A. Kardomateas
Associate Editor